

A 400 solar mass black hole in the Ultraluminous X-ray source M82 X-1 accreting close to its Eddington limit

Dheeraj R. Pasham¹, Tod E. Strohmayer², Richard F. Mushotzky¹

The brightest X-ray source in M82 has been thought to be an intermediate-mass black hole (10^{2-4} solar masses, M_{\odot}) because of its extremely high luminosity and variability characteristics¹⁻⁶, although some models suggest that its mass may be only $\sim 20 M_{\odot}$ ^{3,7}. The previous mass estimates are based on scaling relations which use low-frequency characteristic timescales which have large intrinsic uncertainties^{8,9}. In stellar-mass black holes we know that the high frequency quasi-periodic oscillations that occur in a 3:2 ratio (100-450 Hz) are stable and scale inversely with black hole mass with a reasonably small dispersion¹⁰⁻¹⁵. The discovery of such stable oscillations thus potentially offers an alternative and less ambiguous mass determination for intermediate-mass black holes, but has hitherto not been realized. Here, we report stable, twin-peak (3:2 frequency ratio) X-ray quasi-periodic oscillations from M82 X-1 at the frequencies of 3.32 ± 0.06 Hz and 5.07 ± 0.06 Hz. Assuming that we can scale the stellar-mass relationship, we estimate its black hole mass to be $428 \pm 105 M_{\odot}$. In addition, we can estimate the mass using the relativistic precession model, from which we get a value of $415 \pm 63 M_{\odot}$.

Oscillations arising from general relativistic effects should scale inversely with the black hole mass if they arise from orbital motion near the innermost stable circular orbit in the

¹Astronomy Department, University of Maryland, College Park, MD 20742; email: dheeraj@astro.umd.edu; richard@astro.umd.edu

²Astrophysics Science Division, NASA's Goddard Space Flight Center, Greenbelt, MD 20771; email: tod.strohmayer@nasa.gov

accretion disk^{16,17}, and there is observational support that they do for stellar-mass black holes¹⁰ (3-50 M_{\odot}). M82 X-1’s previous mass estimates of a few hundred solar masses combined with the Type-C identification^{2,4,9} of its mHz X-ray quasi-periodic oscillations suggest that 3:2 ratio, twin-peak, high-frequency oscillations analogous to those seen in stellar-mass black holes, if present, should be detectable in the frequency range of a few Hz¹⁶. We accordingly searched Rossi X-ray Timing Explorer’s (*RXTE*’s) proportional counter array archival data to look for 3:2 oscillation pairs in the frequency range of 1-16 Hz which corresponds to a black hole mass range of 50-2000 M_{\odot} .

We detected two power spectral peaks at 3.32 ± 0.06 Hz (coherence, $Q = \text{centroid frequency } (\nu) / \text{width}(\Delta\nu) > 27$) and 5.07 ± 0.06 Hz ($Q > 40$) consistent with a 3:2 frequency ratio (Fig. 1a, b). The combined statistical significance of the detection is greater than 4.7σ (see Methods for details).

The proportional counter array’s field of view ($1^{\circ} \times 1^{\circ}$) of M82 includes a number of accreting X-ray sources in addition to M82 X-1¹⁸. The remarkable stability of the two quasi-periodic oscillations on timescales of a few years (Movies 1 & 2), their 3:2 frequency ratio and their high oscillation luminosities strongly suggest they are not low-frequency quasi-periodic oscillations from a contaminating stellar-mass black hole (see Methods for details). Also a pulsar origin is very unlikely for several reasons. First, a pulsar signal would be much more coherent than that of the observed quasi-periodic oscillations, which clearly have a finite width. Second, based on the observed high quasi-periodic oscillation luminosities it is extremely implausible that they originate from a pulsar (see Methods for details). Finally, it would be highly coincidental to have two pulsars in the same field of view with spins in the 3:2 ratio. Also, based on the average power spectra of the background sky and a sample of accreting super-massive black holes monitored by the proportional counter array in the same epoch as M82, we rule out an instrumental origin for these oscillations (Extended Data

Figs. 2, 3 & 4). This leaves M82 X-1, persistently the brightest source in the field of view, as the most likely source associated with the 3:2 ratio quasi-periodic oscillation pair.

We estimated M82 X-1’s black hole mass, assuming the $1/M$ (mass) scaling of stellar-mass black holes and the relativistic precession model^{19,20}, to be $428 \pm 105 M_{\odot}$ and $415 \pm 63 M_{\odot}$, respectively (Fig. 2a,b). Combining the average 2-10 keV X-ray luminosity^{21,22} of the source of 5×10^{40} ergs s⁻¹ with the measured mass suggests that the source is accreting close to the Eddington limit with an accretion efficiency of 0.8 ± 0.2 .

The previous mass measurements of M82 X-1 have large uncertainties owing to both systematic and measurement errors. For example, modeling of its X-ray energy spectra during the thermal-dominant state using a fully relativistic multi-colored disk model suggests that it hosts an intermediate-mass black hole with mass anywhere in the range of 200-800 M_{\odot} and accreting near the Eddington limit³. In addition to the large mass uncertainty associated with the modeling, the same study also found that the energy spectra can be equally well-fit with a stellar-mass black hole accreting at a rate of roughly 160 higher than the Eddington limit³. Also, the X-rays from this source are known to modulate with a periodicity of 62 days which has been argued to be the orbital period of an intermediate-mass black hole²²—formed in a nearby star cluster MCG 11 by stellar runaway collisions^{5,23,24}—accreting matter via Roche lobe overflow from a 22-25 M_{\odot} companion star²⁴. Detailed stellar binary evolution simulations suggest that the long periodicity is best explained by an intermediate-mass black hole with mass in the range of 200-5000 M_{\odot} ^{5,24}. But, a recent study finds that this periodicity may instead be due to a precessing accretion disk in which case a stellar-mass black hole will suffice to explain the apparent long periodicity²¹.

One of the main lines of argument for an intermediate-mass black hole in M82 X-1 is by inverse mass scaling of its mHz quasi-periodic oscillations (frequency range of 37-210 mHz^{9,25}; Fig. 1c) to the Type-C low-frequency X-ray oscillations of stellar-mass black holes

(frequency range of 0.2-15 Hz)^{10,26}. There are two uncertainties with such scaling: (1) it was unclear—until now—whether these mHz oscillations are indeed the Type-C analogs of stellar-mass black holes^{8,9} and (2) both the Type-C and the mHz oscillations are variable, resulting in a large dispersion in the measured mass of $25\text{--}1300M_{\odot}$ ^{1,2,4,6}. The discovery of a stable 3:2 high-frequency periodicity simultaneously with the low-frequency mHz oscillations allows for the first time to set the overall frequency scale of the X-ray power spectrum. This result not only asserts that the mHz quasi-periodic oscillations of M82 X-1 are the Type-C analogs of stellar-mass black holes but also provides an independent and the most accurate black hole mass measurement to-date.

Finally, it should be pointed out that while the rms amplitudes (3-5%) of the oscillations reported here and their frequencies with respect to the mHz oscillations (a factor of a few 10s higher) are similar to those observed in stellar-mass black holes¹⁰, they appear narrower (with Q values of 27, 40 & 80) compared to stellar-mass black holes which have Q values of < 20 ^{14,30}. In stellar-mass black holes the Q factor appears to be energy dependent in some cases¹⁴ and it is plausible that a similar effect may be operating in this case.

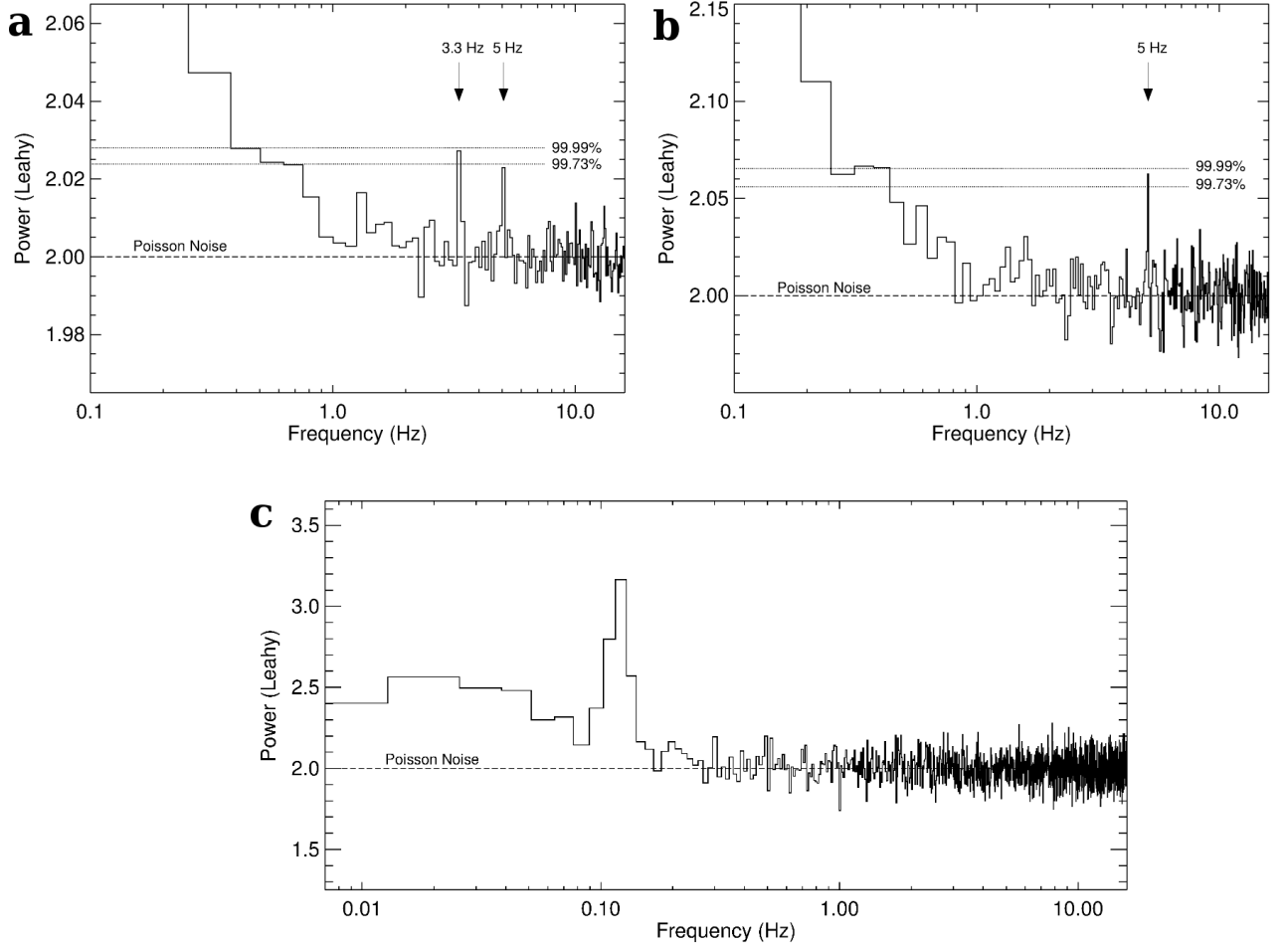


Figure 1 | Power density spectra of M82. (a) Six-year average X-ray (3-13 keV) power density spectrum of M82 using 128-second ($\times 7362$) individual light curves. The frequency resolution is 0.125 Hz. The two strongest features in the power spectrum occur at 3.32 ± 0.06 and 5.07 ± 0.06 Hz consistent with a 3:2 frequency ratio. (b) Averaged power density spectrum of all 1024-second ($\times 363$) segments. The frequency resolution is 0.0625 Hz. The strongest feature is at 5 Hz. (c) For a direct comparison with stellar-mass black holes, we show the broadband power density spectrum of M82 (using ≈ 100 ksecs of *XMM-Newton*/EPIC data; ID: 0206080101) showing the low-frequency quasi-periodic oscillation at 120 mHz in addition to the high-frequency quasi-periodic oscillation pair in the top panels.

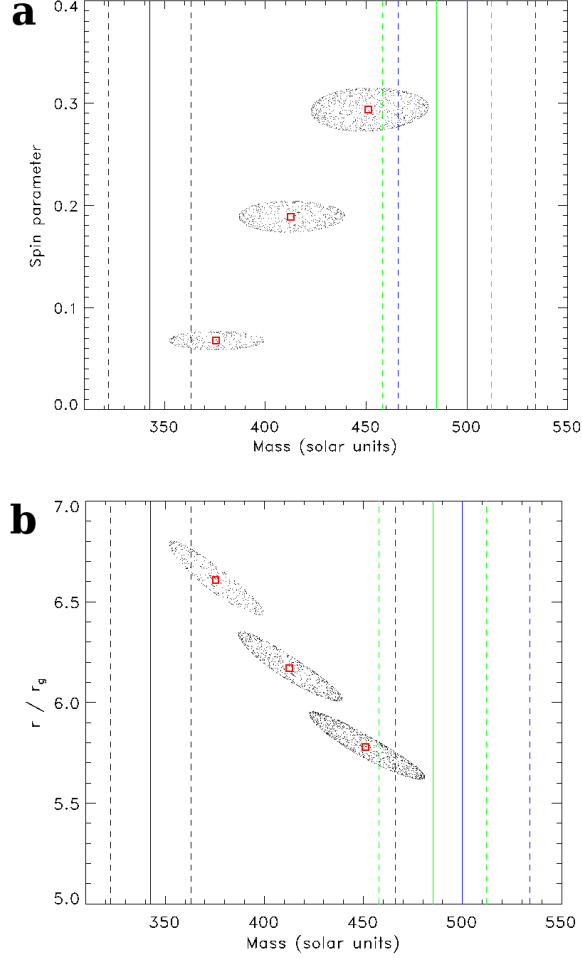
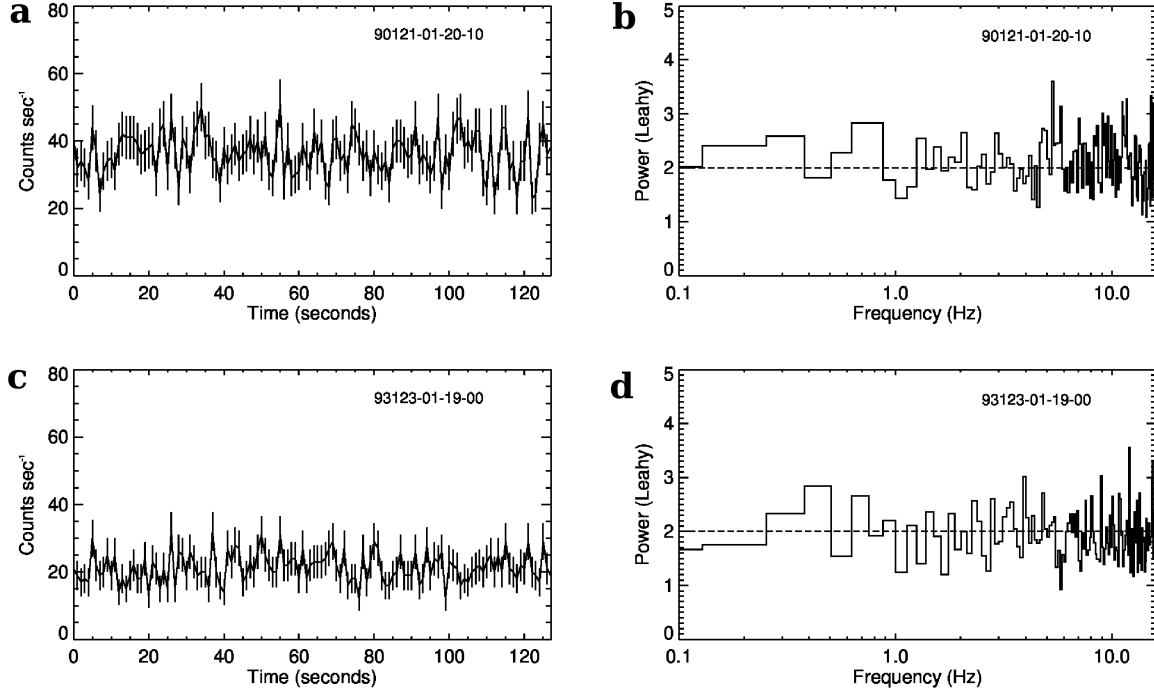
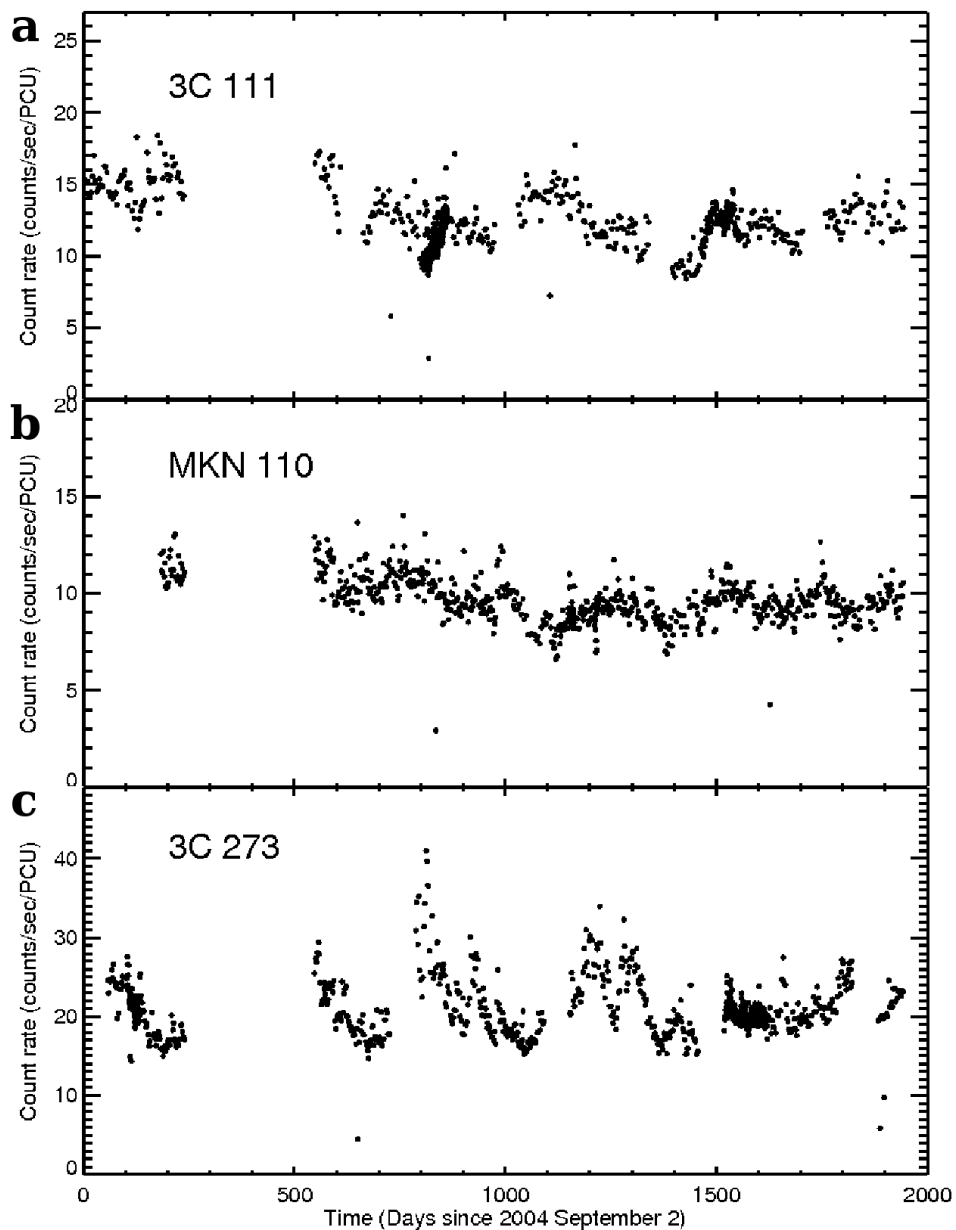


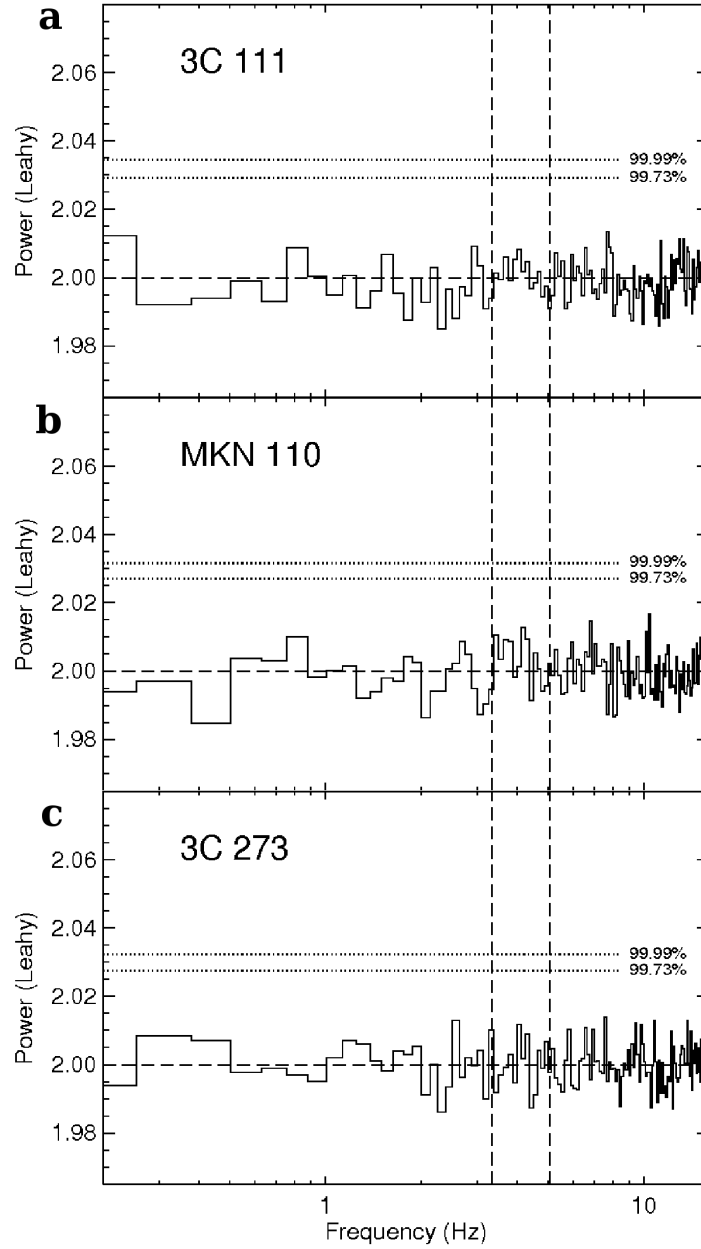
Figure 2 | Mass, spin and radius measurements. (a) Contours (90% confidence) of M82 X-1’s mass as a function of the spin parameter. The three contours correspond to the three low-frequency values (37 mHz, 120 mHz and 210 mHz) with the mass increasing as the low-frequency oscillation frequency increases. (b) Contours of M82 X-1’s mass as a function of the radius of the origin of these oscillations (in units of $r_g = GM/c^2$, where G , M , c are the Gravitational constant, the black hole mass and the speed of light, respectively). In both the panels the vertical lines (solid: solution; dashed: upper-lower limits) represent M82 X-1’s mass estimates assuming a simple $1/M$ scaling for the high-frequency quasi-periodic oscillations. The three colors correspond to scalings using the three microquasars (green: GRO J1655-40²⁷; blue: XTE J1550-64²⁸; black: GRS 1915+105²⁹).



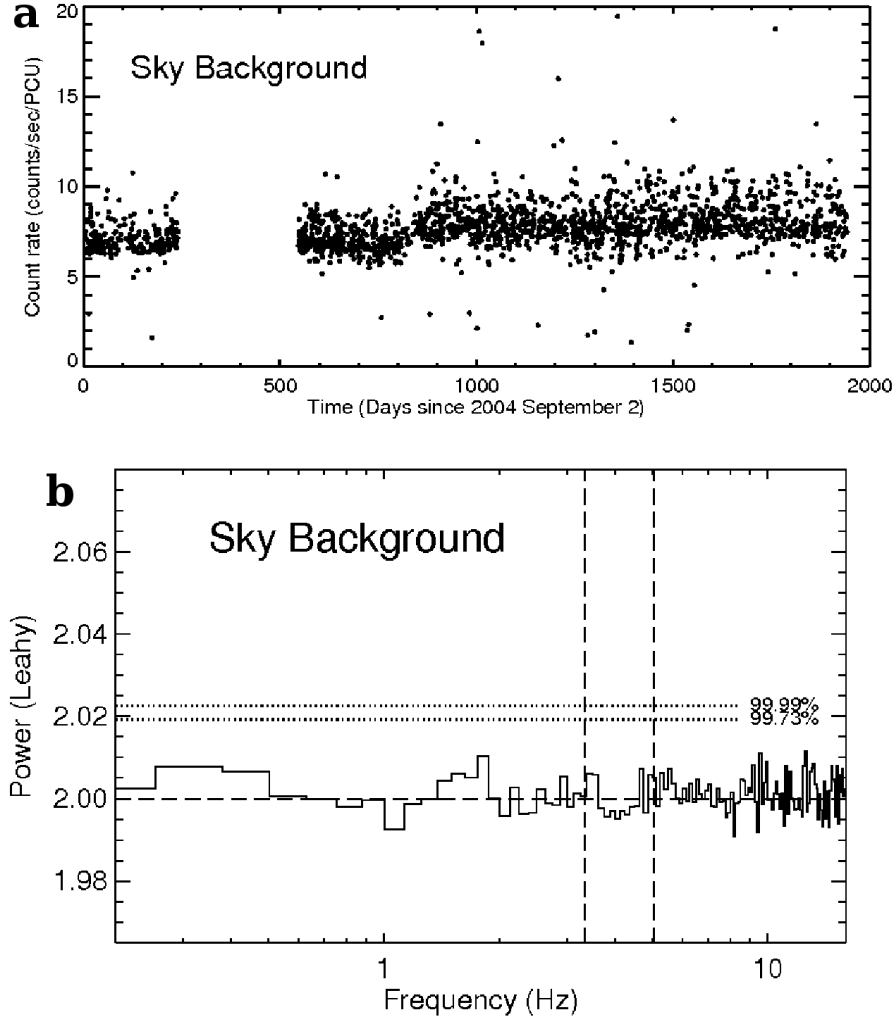
Extended Data Figure 1 | Sample *RXTE* proportional counter array light curves and power density spectra of M82. The 128-second X-ray (3-13 keV) light curves (a, c) and their corresponding power spectra (b, d) of M82. The corresponding observation IDs are shown in the top right of each panel. The light curves have a bin size of 1 second while the power spectra have a frequency resolution of 0.125 Hz. The errorbars in (a, c) represent the standard error on the mean.



Extended Data Figure 2 | Long-term X-ray (3-13 keV) light curves of three accreting super-massive black holes. These were extracted from the same time window as M82 observations (2004 September 02 – 2005 April 30 and 2006 March 03 – 2009 December 30). The name of the galaxy is indicated in the top left of each panel. The count rates are not corrected for background.



Extended Data Figure 3 | Average X-ray (3-13 keV) power spectra of three accreting super-massive black holes. Similar to the M82 analysis, these spectra were extracted by combining all the data (128-second data segments) shown in Extended Data Fig. 2. The Poisson noise level is equal to 2 while the 99.73% and 99.99% confidence contours are indicated by horizontal dotted lines. The two dashed vertical lines are drawn at 3.32 Hz and 5.07 Hz. Clearly, there are no significant power spectral features. The total PCA exposures used for these spectra were 630 ksecs (top), 738 ksecs (middle) and 711 ksecs.



Extended Data Figure 4 | Long-term X-ray (3-13 keV) light curve (top) and the average power density spectrum (bottom) of a background sky field (ra=5.0 deg, dec = -67.0 deg) as observed by *RXTE*/PCA. Similar to the Extended Data Fig. 3 the 99.73% and 99.99% contours and the vertical lines at 3.32 and 5.07 Hz are indicated. Again only observations coincident with M82 monitoring were used (2004 September 02 – 2005 April 30 and 2006 March 03 – 2009 December 30) and the total exposure time was 1450 ksecs.

REFERENCES

1. Casella, P., Ponti, G., Patruno, A., *et al.* Weighing the black holes in ultraluminous X-ray sources through timing. *Mon. Not. R. Astron. Soc.* **387**, 1707-1711 (2008).
2. Dewangan, G. C., Titarchuk, L., & Griffiths, R. E. Black Hole Mass of the Ultraluminous X-Ray Source M82 X-1. *Astrophys. J.* **637**, L21-L24 (2006).
3. Feng, H., & Kaaret, P. Identification of the X-ray Thermal Dominant State in an Ultraluminous X-ray Source in M82. *Astrophys. J.* **712**, L169-L173 (2010).
4. Mucciarelli, P., Casella, P., Belloni, T., Zampieri, L., & Ranalli, P. A variable Quasi-Periodic Oscillation in M82 X-1. Timing and spectral analysis of XMM-Newton and RossiXTE observations. *Mon. Not. R. Astron. Soc.* **365**, 1123-1130 (2006).
5. Patruno, A., Portegies Zwart, S., Dewi, J., & Hopman, C. The ultraluminous X-ray source in M82: an intermediate-mass black hole with a giant companion. *Mon. Not. R. Astron. Soc.* **370**, L6-L9 (2006).
6. Zhou, X.-L., Zhang, S.-N., Wang, D.-X., & Zhu, L. Calibrating the Correlation Between Black Hole Mass and X-ray Variability Amplitude: X-ray Only Black Hole Mass Estimates for Active Galactic Nuclei and Ultra-luminous X-ray Sources. *Astrophys. J.* **710**, 16-23 (2010).
7. Okajima, T., Ebisawa, K., & Kawaguchi, T. A Stellar-Mass Black Hole in the Ultraluminous X-Ray Source M82 X-1? *Astrophys. J.* **652**, L105-L108 (2006).
8. Middleton, M. J., Roberts, T. P., Done, C., & Jackson, F. E. Challenging times: a re-analysis of NGC 5408 X-1. *Mon. Not. R. Astron. Soc.* **411**, 644-652 (2011).
9. Pasham, D. R., & Strohmayer, T. E. On the Nature of the mHz X-Ray Quasi-periodic

- Oscillations from Ultraluminous X-Ray Source M82 X-1: Search for Timing-Spectral Correlations. *Astrophys. J.* **771**, 101-111 (2013).
10. McClintock, J. E., & Remillard, R. A. in Compact stellar X-ray sources (eds Walter Lewin & Michiel van der Klis) 157-213 (Cambridge Univ. Press, 2006).
 11. Remillard, R. A., Morgan, E. H., McClintock, J. E., Bailyn, C. D., & Orosz, J. A. RXTE Observations of 0.1-300 HZ Quasi-periodic Oscillations in the Microquasar GRO J1655-40. *Astrophys. J.* **522**, 397-412 (1999).
 12. Remillard, R. A., Munro, M. P., McClintock, J. E., & Orosz, J. A. Evidence for Harmonic Relationships in the High-Frequency Quasi-periodic Oscillations of XTE J1550-564 and GRO J1655-40. *Astrophys. J.* **580**, 1030-1042 (2002).
 13. Remillard, R. A., Sobczak, G. J., Munro, M. P., & McClintock, J. E. Characterizing the Quasi-periodic Oscillation Behavior of the X-Ray Nova XTE J1550-564. *Astrophys. J.* **564**, 962-973 (2002).
 14. Strohmayer, T. E. Discovery of a 450 HZ Quasi-periodic Oscillation from the Microquasar GRO J1655-40 with the Rossi X-Ray Timing Explorer. *Astrophys. J.* **552**, L49-L53 (2001).
 15. Strohmayer, T. E. Discovery of a Second High-Frequency Quasi-periodic Oscillation from the Microquasar GRS 1915+105. *Astrophys. J.* **554**, L169-L172 (2001).
 16. Abramowicz, M. A., Kluźniak, W., McClintock, J. E., & Remillard, R. A. The Importance of Discovering a 3:2 Twin-Peak Quasi-periodic Oscillation in an Ultraluminous X-Ray Source, or How to Solve the Puzzle of Intermediate-Mass Black Holes. *Astrophys. J.* **609**, L63-L65 (2004).

17. Abramowicz, M. A., & Kluźniak, W. Interpreting black hole QPOs. *X-ray Timing 2003: Rossi and Beyond*. **714**, 21-28 (2004).
18. Matsumoto, H., Tsuru, T. G., Koyama, K., *et al.* Discovery of a Luminous, Variable, Off-Center Source in the Nucleus of M82 with the Chandra High-Resolution Camera. *Astrophys. J.* **547**, L25-L28 (2001).
19. Stella, L., Vietri, M., & Morsink, S. M. Correlations in the Quasi-periodic Oscillation Frequencies of Low-Mass X-Ray Binaries and the Relativistic Precession Model. *Astrophys. J.* **524**, L63-L66 (1999).
20. Motta, S. E., Belloni, T. M., Stella, L., Muñoz-Darias, T., & Fender, R. Precise mass and spin measurements for a stellar-mass black hole through X-ray timing: the case of GRO J1655-40. *Mon. Not. R. Astron. Soc.* **437**, 2554-2565 (2014).
21. Pasham, D. R., & Strohmayer, T. E. Can the 62 Day X-Ray Period of ULX M82 X-1 Be Due to a Precessing Accretion Disk? *Astrophys. J.* **774**, L16-L22 (2013).
22. Kaaret, P., & Feng, H. Confirmation of the 62 Day X-Ray Periodicity from M82. *Astrophys. J.* **669**, 106-108 (2007).
23. Voss, R., Nielsen, M. T. B., Nelemans, G., Fraser, M., & Smartt, S. J. On the association of ULXs with young superclusters: M82 X-1 and a new candidate in NGC 7479, *Mon. Not. R. Astron. Soc.* **418**, L124 (2011).
24. Portegies Zwart, S. F., Baumgardt, H., Hut, P., Makino, J., & McMillan, S. L. W. Formation of massive black holes through runaway collisions in dense young star clusters. *Nature*. **428**, 724 (2004).
25. Caballero-García, M. D., Belloni, T., & Zampieri, L. Quasi-periodic oscillations and

- energy spectra from the two brightest Ultra-Luminous X-ray sources in M82. *Mon. Not. R. Astron. Soc.* **436**, 3262-3270 (2013).
26. Casella, P., Belloni, T., & Stella, L. The ABC of Low-Frequency Quasi-periodic Oscillations in Black Hole Candidates: Analogies with Z Sources. *Astrophys. J.* **629**, 403-407 (2005).
 27. Beer, M. E., & Podsiadlowski, P. The quiescent light curve and the evolutionary state of GRO J1655-40. *Mon. Not. R. Astron. Soc.* **331**, 351-360 (2002).
 28. Orosz, J. A., Steiner, J. F., McClintock, J. E., *et al.* An Improved Dynamical Model for the Microquasar XTE J1550-564. *Astrophys. J.* **730**, 75-88 (2011).
 29. Steeghs, D., McClintock, J. E., Parsons, S. G., *et al.* The Not-so-massive Black Hole in the Microquasar GRS1915+105. *Astrophys. J.* **768**, 185-192 (2013).
 30. Belloni, T. M., Sanna, A., & Méndez, M. High-frequency quasi-periodic oscillations in black hole binaries. *Mon. Not. R. Astron. Soc.* **426**, 1701-1709 (2012).

Acknowledgements This work is based on observations made with the Rossi X-ray Timing Explorer (*RXTE*), a mission that was managed and controlled by NASA’s Goddard Space Flight Center (GSFC) in Greenbelt, Maryland, USA. All the data used in the present article is publicly available through NASA’s *HEASARC* archive. Pasham would like to thank Margaret Trippe, Cole Miller and Chris Reynolds for valuable discussions. Finally, we would like to thank the referee for suggesting to check for pulsations in PCA’s AGN data.

Author contributions Dheeraj R. Pasham and Tod E. Strohmayer both reduced the data and carried out the analysis. They also wrote the paper. Richard F. Mushotzky contributed towards the interpretation of the results.

Author information Reprints and permissions information is available at www.nature.com/reprints. The authors declare no competing financial interests. Correspondence and requests for materials should be addressed to dheeraj@astro.umd.edu.

Methods

Estimating the expected significance of the quasi-periodic oscillations. The detectability (statistical significance, n_σ) of a quasi-periodic oscillation feature can be expressed as,

$$n_\sigma = \frac{1}{2} r^2 \frac{S^2}{(S+B)} \sqrt{\frac{T}{\Delta\nu}}, \quad (1)$$

where r , S , B , T , and $\Delta\nu$ are the rms (root-mean-squared) amplitude of the quasi-periodic oscillation, the source count rate, the background count rate, the exposure time, and the width of the quasi-periodic oscillation, respectively³¹. Assuming an rms amplitude of a few percent—similar to that seen in stellar-mass black holes³⁰—and using the mean *RXTE* proportional counter array source and background rates obtained from prior observations²¹, we found that the wealth of publicly available, archival *RXTE* monitoring data (≈ 1 Megasecond) spread across a timespan of ≈ 6 years would provide a sensitive search for high-frequency quasi-periodic oscillations in M82 X-1.

Data primer. M82 was monitored (0.5-2 ksecs roughly once every three days) with the Rossi X-ray Timing Explorer’s (*RXTE*’s) proportional counter array (*PCA*) between 1997 February 2 until 1997 November 25 (0.8 years) and 2004 September 2 until 2009 December 30 (5.3 years). All the *PCA* observations were carried out in the *GoodXenon* data acquisition mode. The total number of monitoring observations was 867, which were divided amongst six proposals (*RXTE* proposal IDs: P20303, P90121, P90171, P92098, P93123, P94123). As recommended by the data analysis guide provided by the *RXTE* Guest Observer Facility (GOF) (<https://heasarc.gsfc.nasa.gov/docs/xte/abc/screening.html>), we first screened the data to only include time intervals that satisfy the following criteria: $\text{ELV} > 10.0$ && $\text{OFF-SET} < 0.02$ && $(\text{TIME_SINCE_SAA} < 0 \parallel \text{TIME_SINCE_SAA} > 30)$ && $\text{ELECTRON2} < 0.1$. In addition to the above standard filters, we only used X-ray events within the energy range of 3-13 keV which translates to *PCA* channels 7-32. This energy range is comparable

to the bandpass in which high-frequency quasi-periodic oscillations have been reported from stellar-mass black holes^{10,14,15}. Moreover, beyond 13 keV the background dominates the overall count rate by a factor greater than 10. For each observation we used all active proportional counter units (PCUs) in order to maximize the count rate, and thus the sensitivity to quasi-periodic oscillations.

Before we extracted the individual power spectra we created individual light curves (using a bin size of 1 second) from all the observations. Through manual inspection we removed a small number of observations affected by flares, as these are attributed to background events not associated with the source, for example, gamma-ray bursts. Extended Data Fig. 1 shows two sample light curves and their corresponding power spectra. They represent the typical quality of the individual light curves used in extracting the average power spectra.

Estimating the statistical significances. We first divided the data into 128-second segments and extracted their light curves with a time resolution of 1/32 seconds. We then constructed a Leahy normalized³² power density spectrum (where the Poisson noise level is 2) from each of these 128-second light curves. All the power spectra were then combined (7362 individual power spectra) to obtain a six-year averaged power density spectrum of M82 (Fig. 1a).

In order to estimate the statistical significance of any features in the 1-16 Hz range of the six-year averaged power density spectrum obtained using the 128-second data segments, we first ensured that the local mean was equal to 2, the value expected from a purely Poisson (white noise) process. We then computed the probability, at the 99.73% (3σ) and the 99.99% (3.9σ) confidence levels, of obtaining the power, $P = P_* \times 7362 \times 16$ from a χ^2 distribution with $2 \times 7362 \times 16$ degrees of freedom. Here P_* is the power value of a statistical fluctuation at a given confidence level. We used this χ^2 distribution because we averaged in frequency by a factor of 16 and averaged 7362 individual power spectra. Considering the total number

of trials (frequency bins within 1-16 Hz) we computed the 99.73% ($1/(371 \times \text{trials})$) and the 99.99% ($1/(10000 \times \text{trials})$) confidence limits (horizontal dotted lines in Fig. 1a). We detect two power spectral peaks at 3.32 ± 0.06 Hz and 5.07 ± 0.06 Hz significant at the 2×10^{-4} (3.7σ) and 6×10^{-3} (2.75σ) levels, respectively, assuming both features were searched for independently between 1-16 Hz. However, after identifying the first feature at 3.3 Hz, if we are searching for a second feature at a 3:2 ratio, then the search from thereon only includes the bins nearby $3/2$ or $2/3$ of 3.3 Hz. If this is taken into consideration the significance of the 5 Hz feature increases due to the smaller number of trials to 5×10^{-4} or 3.5σ . In order to further test the significance of the 5 Hz feature, we extracted an average power density spectrum using all the data with segments longer than 1024 seconds (Fig. 1b). The 5 Hz feature ($Q > 80$) is clearly detected at the 1.5×10^{-4} confidence level or 3.8σ , considering a full search between 1-16 Hz.

The combined probability of two independent chance fluctuations—in the 3:2 frequency ratio—one at the 3.7σ level (3.3 Hz feature) and the other at the 2.75σ level (5 Hz feature) is greater than 4.7σ .

Signal cannot be from a single observation. The very presence of these two features in the six-year averaged power spectrum suggests that they are stable on this timescale. In order to further rule out the possibility that these oscillations are due to a single or small number of particular observations, we constructed two dynamic average power spectra, one for the 128-second segments (dynamic power density spectrum#1 or Movie 1) and another for the 1024-second segments (dynamic power density spectrum#2 or Movie 2). These track the evolution of the average power density spectra as a function of the total number of individual power spectra used in constructing the average. The two dynamic power density spectra clearly suggest that the power in these two features builds-up gradually as more data is being averaged, as opposed to a sudden appearance, which would be expected if a

single or a small number of observations were contributing all the signal power. In addition, dynamic power density spectrum#1 clearly shows that while the 5 Hz feature is stronger during the earlier stages of the monitoring program the 3.3 Hz feature is stronger during the later observations. Longer exposures of the order of 1-2 ksecs were carried out during the earlier stage of the monitoring program, which explains the higher significance of the 5 Hz feature in the average power density spectrum of the 1024-second segments (Fig. 1b).

RMS amplitude of the quasi-periodic oscillations. To calculate the rms variability amplitude of these quasi-periodic oscillations we first determined the mean net count rate (source + background) of all the light curves used to extract the average power spectra. These values were equal to 29.9 counts s⁻¹ and 35.2 counts s⁻¹ for the 128-second and the 1024-second segment power spectra, respectively. The rms amplitudes of the 3.3 Hz and the 5 Hz quasi-periodic oscillations, not correcting for the background, were estimated to be 1.1±0.1% and 1.0±0.1%, respectively. Similarly, the rms amplitude of the 5 Hz feature within the 1024-second segment power density spectrum was estimated to be 1.1±0.1%. We then estimated the mean background count rate from the *Standard2* data utilizing the latest *PCA* background model. The mean background rates during the 128-second and the 1024-second segments were estimated to be 18.9 counts s⁻¹ and 24.0 counts s⁻¹, respectively. After accounting for the X-ray background we find that the rms amplitudes of the 3.3 Hz and the 5 Hz features—averaged over the entire data—are 3.0±0.4% and 2.7±0.4%, respectively, while the amplitude of the 5 Hz feature within the 1024-second power density spectrum was estimated to be 3.5±0.4%.

Furthermore, the source count rates estimated above (*net* minus *background*) represent the combined contribution from all the X-ray point sources within the *PCA*'s 1°×1° field of view¹⁸. Thus, the quasi-periodic oscillation rms amplitudes are underestimated. A study using the high-resolution camera (HRC) on board *Chandra* suggests that there are multiple

point sources within the $1' \times 1'$ region around M82 X-1^{18,33}. Tracking the long-term variability of these sources suggests that the maximum luminosity reached by any of these sources—except for source 5 (as defined by ref. 18)—is less than $1/5^{th}$ of the average luminosity of M82 X-1³³. Source 5 is a highly variable transient ULX with its 0.5-10 keV luminosity varying between 10^{37-40} ergs s⁻¹ (see the middle-left panel of Fig. 1 of ref. 33). The quasi-periodic oscillations reported here are most likely produced from M82 X-1, which has persistently been the brightest source of any in the immediate vicinity of M82 X-1 (see the following sections). Although a precise value of the rms amplitude cannot be evaluated using the current data, we estimate an absolute upper limit by calculating the inverse of the fraction of the count rate contribution from M82 X-1, assuming all the remaining contaminating sources are at their brightest ever detected. This scenario is highly unlikely but will serve as an absolute upper bound to the rms amplitudes of the quasi-periodic oscillations, assuming they are from M82 X-1. Using the values reported by ref. 33 the fraction is roughly 1.8. Thus the true rms amplitudes of the 3.3 Hz and the 5 Hz quasi-periodic oscillations are estimated to be in the range of 3-5%.

Also, *XMM-Newton*'s EPIC instruments – with an effective area of $\approx 1/5^{th}$ of *RXTE*'s *PCA* albeit with lower background – observed M82 on multiple epochs, with a total effective exposure of ≈ 350 ksecs. These observations were taken in the so-called full-frame data acquisition mode with a time resolution of 73.4 ms or a Nyquist frequency of 6.82 Hz. This value is close to the quasi-periodic oscillation frequencies of interest and causes some signal suppression³¹. Nevertheless, we extracted an average 3-10 keV power density spectrum with 128-second data segments using all the observations (2718 individual power spectra). We do not detect any statistically significant features nearby 3.3 and 5 Hz, however, we estimate a quasi-periodic oscillation upper limit (3σ confidence) of 5.2 and 6.2% rms (using Eq. 4.4 and Eq. 4.10 of ref. 28) at 3.3 and 5 Hz, respectively, which are roughly twice the rms values of the quasi-periodic oscillations detected in the *PCA* data.

Using the 128-second data segments from *RXTE*, we also studied the energy dependence of the rms amplitudes of the two oscillations (see Extended Data Table 1). While the error bars are large, there appears to be a modest decrease in the rms amplitudes of these oscillations at lower X-ray energies. *XMM-Newton*’s EPIC instruments are more sensitive in the 3-8 keV band which is comparable to the PCA channels of 7-18 (the first and the fourth rows of the Extended Data Table 1).

Ruling out low-frequency quasi-periodic oscillations. Low-frequency quasi-periodic oscillations of stellar-mass black holes, such as the Type-C quasi-periodic oscillations²⁶, have typical centroid frequencies of a few Hz with rms amplitudes²⁶ of 5-25%, but are known to vary in frequency by factors of 8-10 over time scales of days^{34,35}. This would lead to very broad features in the kind of average power spectra we have computed from. Moreover, among the plethora of low-frequency quasi-periodic oscillations currently known there is no indication of them preferentially occurring with a 3:2 frequency ratio. Furthermore, the average luminosity of the quasi-periodic oscillations reported here is $\approx 0.03 \times$ (the average luminosity of all the sources observed by the *PCA* in the 3-13 keV band)^{21,22} which is $\approx 0.03 \times 5 \times 10^{40} \text{ ergs s}^{-1} = 1.5 \times 10^{39} \text{ ergs s}^{-1}$. This is comparable to or more than the peak X-ray luminosities of the contaminating sources, except for source 5^{33,36}. Therefore, if these features were simply low-frequency quasi-periodic oscillations produced by any of the contaminating sources—except for source 5—their X-ray flux would have to be modulated at almost 100%, which is not plausible for the typical amplitudes of low-frequency quasi-periodic oscillations.

Source 5, which is a ULX, could in principle be the origin of these 3:2 ratio quasi-periodic oscillations. However, 3-4 mHz quasi-periodic oscillations have been discovered from this source and have been identified as Type-A/B quasi-periodic oscillations analogs of stellar-mass black holes³⁷. Such a characterization for the mHz quasi-periodic oscillations

suggests that the ULX might host a black hole with a mass of 12,000-43,000 M_{\odot} ³⁷. If that were the case, the expected frequency range of high-frequency quasi-periodic oscillation analogs for a few 10,000 M_{\odot} black hole would be a few 100s of mHz, a factor of 10 lower than the quasi-periodic oscillations reported here, thus suggesting that the 3.3 and 5 Hz quasi-periodic oscillations are less likely to be the high-frequency quasi-periodic oscillation analogs of source 5.

Ruling out pulsar origin. Rotation-powered pulsars can be strongly excluded, they simply cannot provide the required luminosity. A neutron star’s rotational energy loss rate can be expressed in terms of its moment of inertia, I , spin period P , and period derivative, \dot{P} as,

$$\dot{E}_{rot} = \frac{2\pi^2 I \dot{P}}{P^3}. \quad (2)$$

No known pulsar has a spin-down luminosity comparable to the estimated quasi-periodic oscillation X-ray luminosity. For example, the energetic Crab pulsar has $\dot{E} \approx 2 \times 10^{38}$ ergs s^{-1} , and only a fraction of a pulsar’s spin-down power typically appears as X-ray radiation. This rules out rotation-powered pulsars. As M82 is a starburst galaxy it likely hosts a population of accreting X-ray pulsars. Such accretion-powered pulsar systems are typically limited by the Eddington limit of $\approx 2 \times 10^{38}$ ergs s^{-1} for a “canonical” neutron star. Useful comparisons can be made with the population observed with the *RXTE/PCA* in the Small Magellanic Cloud (SMC)³⁸. These authors present pulsed luminosities for the SMC pulsar population, and none is larger than $\approx 3 \times 10^{38}$ ergs s^{-1} . Again, this is much smaller than the inferred quasi-periodic oscillations luminosities. Moreover, such pulsars are variable, and their time-averaged luminosities would be reduced further by their outburst duty cycles. At present the only pulsar that is known to reach luminosities of $\sim 10^{40}$ ergs s^{-1} for brief periods of time is GRO J1744-28—the so-called bursting pulsar^{39–41}. This object has a 2.1 Hz spin frequency and was discovered during an outburst that spanned the first 3 months of 1996 (we note that at the time of writing the source was detected in outburst again, suggesting

a duty cycle of about 18 years, ATel #5790, #5810, #5845, #5858, #5883, #5901). It's peak persistent luminosity (assuming a distance close to that of the Galactic center) was $\approx 7 \times 10^{38}$ ergs s $^{-1}$. With a pulsed amplitude of about 10% this would still give a pulsed luminosity much less than the inferred luminosities of the quasi-periodic oscillations. The Type II-accretion driven-bursts from this source⁴² could reach about 10^{40} ergs s $^{-1}$, and with a 10% pulsed amplitude this could give an instantaneous luminosity close to that of the average quasi-periodic oscillation luminosities. However, the bursting intervals make up less than 1% of the total time, and thus this small duty cycle will reduce the average pulsed luminosity due to the bursts to a level substantially below that of the observed quasi-periodic oscillations. Thus, we conclude that the observed quasi-periodic oscillations cannot be associated with accreting pulsars in M82.

Ruling out instrumental origin. We also rule out the possibility that this signal is intrinsic to *RXTE*/PCA by extracting the average power density spectra of a sample of accreting super-massive black holes with PCA count rates comparable to M82. To be consistent we only used monitoring data taken in the *GoodXenon* mode during the same epoch as M82. The long-term light curves of these sources in the same time range as M82 are shown in the Extended Data Fig. 2. Based on the causality argument active galactic nuclei with black hole masses greater than $10^6 M_{\odot}$ cannot have coherent oscillations at frequencies higher than ≈ 0.1 Hz. The average power spectra obtained with PCA in the 3-13 keV bandpass are essentially flat and are consistent with being Poisson noise (see Extended Data Fig. 3). In addition, we also extracted the average power spectrum of a blank sky field (background) monitored using the *GoodXenon* mode during the same epoch as M82. The corresponding average power spectrum is shown in the Extended Data Fig. 4b and is again consistent with being featureless, as expected.

Relativistic precession model analysis. Under the interpretation of the relativistic

precession model (RPM), the upper harmonic of the high-frequency quasi-periodic oscillation is associated with the Keplerian frequency at some inner radius while the lower harmonic of the high-frequency quasi-periodic oscillation and the Type-C quasi-periodic oscillation are associated with the periastron and nodal precession frequencies, respectively, at the same radius. Recently, ref. 20 have applied this model to GRO J1655-40 which exhibits both the low-frequency and the high-frequency quasi-periodic oscillations and has a very accurate mass measurement of $5.4 \pm 0.3 M_{\odot}$ ²⁷. They find that the black hole mass evaluated from the relativistic precession model analysis agrees nicely with its dynamical mass estimate. Given this promise of the relativistic precession model, we estimated the mass and spin of M82 X-1's black hole using this model and essentially following the methodology as in ref. 20.

The relativistic precession model analysis requires that the three quasi-periodic oscillations, the two high-frequency quasi-periodic oscillations and a low-frequency quasi-periodic oscillation, be observed simultaneously. This is however not the case for M82 observations. While the combined six-year *RXTE*'s proportional counter array data shows the twin high-frequency quasi-periodic oscillation pair, individual *XMM-Newton* observations randomly dispersed over the same epoch as the *RXTE* monitoring have shown mHz low-frequency quasi-periodic oscillations with frequencies in the range of 37-210 mHz (see Table 2 of ref. 10 and ref. 23). Thus, we carried out the analysis for three separate values of the low-frequency quasi-periodic oscillations, the lowest and the highest values of 37 mHz and 210 mHz, respectively, as well as a mean quasi-periodic oscillation frequency of 120 mHz.

The dimensionless spin parameter is constrained to the range $0.06 < a < 0.31$, and the inferred radius, r , in the disk is in the range $5.53 < r/r_g < 6.82$, where $r_g = GM/c^2$ (G and c are the gravitational constant and the speed of light, respectively, while M is the mass of the black hole).

REFERENCES

- 31. van der Klis, M. in Timing Neutron Stars: proc. of the NATO Adv. Study Inst. on Timing Neutron Stars (eds H. Ogelman & E. P. J. van den Heuvel) 27 (Kluwer Academic / Plenum Publishers, 1989)
- 32. Leahy, D. A., Darbro, W., Elsner, R. F., *et al.* On searches for pulsed emission with application to four globular cluster X-ray sources - NGC 1851, 6441, 6624, and 6712. *Astrophys. J.* **266**, 160-170 (1983).
- 33. Chiang, Y.-K., & Kong, A. K. H. The long-term variability of the X-ray sources in M82. *Mon. Not. R. Astron. Soc.* **414**, 1329-1338 (2011).
- 34. Wood, K. S., Ray, P. S., Bandyopadhyay, R. M., *et al.* USA Experiment and RXTE Observations of a Variable Low-Frequency Quasi-periodic Oscillation in XTE J1118+480. *Astrophys. J.* **544**, L45-L48 (2000).
- 35. Rodriguez, J., Corbel, S., Kalemci, E., Tomsick, J. A., & Tagger, M. An X-Ray Timing Study of XTE J1550-564: Evolution of the Low-Frequency Quasi-periodic Oscillations for the Complete 2000 Outburst. *Astrophys. J.* **612**, 1018-1025 (2004).
- 36. Jin, J., Feng, H., & Kaaret, P. Transition to the Disk Dominant State of a New Ultraluminous X-ray Source in M82. *Astrophys. J.* **716**, 181-186 (2010).
- 37. Feng, H., Rao, F., & Kaaret, P. Discovery of Millihertz X-Ray Oscillations in a Transient Ultraluminous X-Ray Source in M82. *Astrophys. J.* **710**, L137-L141 (2010).
- 38. Laycock, S., Corbet, R. H. D., Coe, M. J., *et al.* Long-Term Behavior of X-Ray Pulsars in the Small Magellanic Cloud. *Astrophys. J.* **161**, 96-117 (2005).
- 39. Giles, A. B., Swank, J. H., Jahoda, K., *et al.* The Main Characteristics of GRO J1744-28

- Observed by the Proportional Counter Array Experiment on the Rossi X-Ray Timing Explorer. *Astrophys. J.* **469**, L25 (1996).
40. Jahoda, K., Stark, M. J., Strohmayer, T. E., *et al.* Peak luminosities of bursts from GRO J1744-28 measured with the RXTE PCA. *Nucl. Phys. B Proc. Suppl.* **69**, 210-215 (1999).
41. Sazonov, S. Y., Sunyaev, R. A., & Lund, N. Super-Eddington x-ray luminosity of the bursting pulsar GRO J1744-28: WATCH/Granat observations. *Astron. Letters* **23**, 286-292 (1997).
42. Kommers, J. M., Fox, D. W., Lewin, W. H. G., *et al.* Postburst Quasi-periodic Oscillations from GRO J1744-28 and from the Rapid Burster. *Astrophys. J.* **482**, L53 (1997).

Extended Data Table 1 | Dependence of the % rms amplitudes of the two oscillations on X-ray bandpass[†].

PCA Channels	Energy Range	Net Count Rate ^a	Background Count Rate	Uncorrected % rms Amplitude ^b	Corrected % rms Amplitude ^c
3.32 Hz Quasi-Periodic Oscillation					
7-18	3-8 keV	19.0	10.5	1.1±0.2	2.8±0.4
7-24	3-10 keV	24.3	14.5	1.1±0.2	2.5±0.4
7-32	3-13 keV	29.9	18.9	1.1±0.1	2.7±0.4
5.07 Hz Quasi-Periodic Oscillation					
7-18	3-8 keV	19.0	10.5	1.2±0.2	2.5±0.4
7-24	3-10 keV	24.3	14.5	1.0±0.2	2.8±0.4
7-32	3-13 keV	29.9	18.9	1.0±0.1	3.0±0.4

[†]We used 128-second data segments for this study. ^aThe total (source + background) count rate in the given energy range.

^bNot corrected for the background. ^cBackground corrected % rms amplitude where corrected rms amplitude = (uncorrected rms amplitude)×(Total Count Rate)/(Source Count Rate). The source count rate is simple the total minus the background rate.